




# A rotating sample cell for *in situ* measurements of adsorption with x-rays

Cite as: Rev. Sci. Instrum. **89**, 123113 (2018); <https://doi.org/10.1063/1.5053860>

Submitted: 27 August 2018 . Accepted: 05 December 2018 . Published Online: 26 December 2018

Ramonna I. Kosheleva , Athanasios T. Varoutoglou, George A. Bomis, George Z. Kyzas , Evangelos P. Favvas, and Athanasios Ch. Mitropoulos 



View Online



Export Citation



CrossMark

## ARTICLES YOU MAY BE INTERESTED IN

[A high beam energy photoelectron-photofragment coincidence spectrometer for complex anions](#)



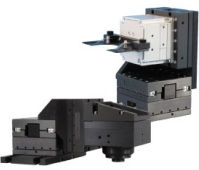
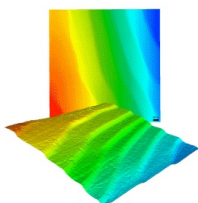
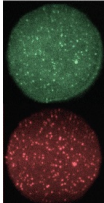
Review of Scientific Instruments **89**, 123304 (2018); <https://doi.org/10.1063/1.5074112>

[Contributed Review: A review of compact interferometers](#)

Review of Scientific Instruments **89**, 121501 (2018); <https://doi.org/10.1063/1.5052042>

[Capillary-tube package devices for the quantitative performance evaluation of nuclear magnetic resonance spectrometers and pulse sequences](#)

Review of Scientific Instruments **89**, 123115 (2018); <https://doi.org/10.1063/1.5052374>

 <b>MCL</b> MAD CITY LABS INC. <a href="http://www.madcitylabs.com">www.madcitylabs.com</a>	<p>Nanopositioning Systems</p> 	<p>Modular Motion Control</p> 	<p>AFM and NSOM Instruments</p> 	<p>Single Molecule Microscopes</p> 
---	--	--	---	--

## A rotating sample cell for *in situ* measurements of adsorption with x-rays

Ramonna I. Kosheleva,<sup>1,2</sup> Athanasios T. Varoutoglou,<sup>1</sup> George A. Bomis,<sup>1</sup> George Z. Kyzas,<sup>1</sup> Evangelos P. Favvas,<sup>3</sup> and Athanasios Ch. Mitropoulos<sup>1,a)</sup>

<sup>1</sup>*Hephaestus Laboratory, Department of Petroleum and Mechanical Engineering, Eastern Macedonia and Thrace Institute of Technology, St. Lucas, 654 04 Kavala, Greece*

<sup>2</sup>*Faculty of Chemistry, Division of Chemical Technology, Aristotle University of Thessaloniki, University Box 116, 54124 Thessaloniki, Greece*

<sup>3</sup>*Membranes and Materials for Environmental Separations Laboratory, Institute of Nanoscience and Nanotechnology, NCSR "Demokritos" Ag. Paraskevi, Attica 153 41, Greece*

(Received 27 August 2018; accepted 5 December 2018; published online 26 December 2018)

A sample cell which facilitates adsorption in conjunction with small angle x-ray scattering under a rotational field is presented. The device allows dynamic phenomena that take place within a pore system to be investigated *in situ* by x-rays. As an example, a sample of Vycor porous glass was measured at relative pressures  $p/p_0 = 0$  and  $p/p_0 = 0.5$ . For the static measurements, the results were as expected. Under rotation, an increase in the scattered intensity of the loaded sample, over the corresponding static one, is observed. Fractal analysis has shown an increase in the fractal dimension even higher than that of the dry sample. It was suggested that the increase in the scattered intensity was due to the rotation, while the abnormality in the fractal dimension was due to asymmetric ripples of the adsorbed layers. The limits of the technique are given too. *Published by AIP Publishing.* <https://doi.org/10.1063/1.5053860>

### INTRODUCTION

Rotation can intensify a number of industrial processes resulting in an increase in production efficiency and a decrease in energy consumption and environmental footprint. Several studies have focused on rotating packed beds;<sup>1–10</sup> however, from the case of a single gas in a rotating cylinder to a more complex situation of liquid-gas interaction in a porous interface, the involved mechanisms are poorly understood.

In an early study, de Socio *et al.*<sup>11</sup> had drawn an analytical solution for the molecular flow between two concentric rotating cylinders, in a rarefied gas dynamics reference frame, for the one-dimensional problem. In the same work, they have also indicated the difficulties in approximating analytic solutions for the general case. Later on, Geyko and Fisch<sup>12</sup> discussed the behavior of an ideal spinning gas in a rotating cylinder. They have concluded that under compression, parallel to the axis of rotation, the spinning gas exhibits reduced compressibility and other unusual properties. Recently, Gao *et al.*<sup>13</sup> investigated gas flow characteristics in a rotating packed bed, of rotating speed between 100 and 300 rpm, by particle image velocimetry. They found that the turbulent kinetic energy near the inner packing was higher than those in the bulk zone, indicating the existence of the gas end-effect. It was suggested that a further study on gas/solid or gas/liquid interface is necessary.

Small angle x-ray scattering<sup>14</sup> (SAXS) is an advanced characterization method that may help to gain a deeper insight into the aforementioned occurring processes, especially if it is combined with appropriate *in situ* techniques. For an isotropic porous medium, the spherically averaged intensity  $I(Q)$  is

given as

$$I(Q) = 4\pi\rho^2V \int_0^\infty r^2\gamma(r) \frac{\sin Qr}{r} dr, \quad (1)$$

where  $V$  is the volume of the sample,  $\rho$  is the electron density,  $\gamma(r)$  is the correlation function at point  $r$ , and  $Q$  is the scattering vector;  $Q = 4\pi \sin \theta/\lambda$ , where  $\lambda$  is the wavelength and  $2\theta$  is the scattering angle.

Within certain regions, Eq. (1) may be reduced to simpler forms from which information on the pore size and surface area may be obtained. For instance, the outer part of the spectrum (i.e., at high  $Q$ ) commonly decays by following a power law of slope =  $-4$ , known as Porod's law. When, however, the texture of the surface is not smooth, there will be deviations from this law which may be interpreted as a fractally rough surface with a fractal dimension  $D = 6 - |\text{slope}|$ .<sup>15</sup>

Small angle x-ray scattering in conjunction with adsorption can provide information not only on the structural details of the porous medium but also on the physical processes involved within the pore matrix.<sup>16–18</sup> In the case of a two phase system,  $I(Q)$  is equal to

$$I(Q) = I_{00}(\rho_1 - \rho_2)^2, \quad (2)$$

where  $I_{00}$  is a constant and  $\rho_1$  and  $\rho_2$  are the electron densities of the two phases. When those densities come equal, the scattered intensity will be zero and contrast matching will be reached. During adsorption, an adsorbed film is first deposited on the pore walls and then capillary condensation takes place within certain classes of pores which satisfies the Kelvin equation<sup>19</sup> at that relative pressure ( $p/p_0$ ). The condensed class of pores will cease to act as a scatterer, and only the remaining empty pores will produce a measurable intensity; as a result, a drop in  $I(Q)$  will be observed. From

<sup>a)</sup> Author to whom correspondence should be addressed: amitrop@teiimt.gr

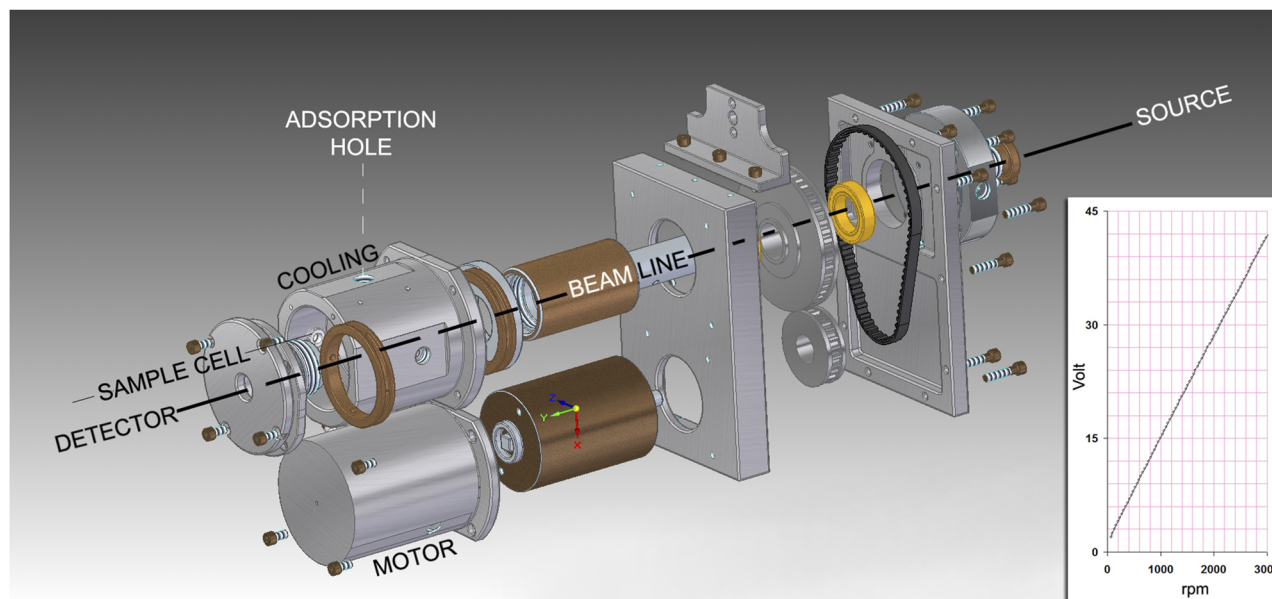


FIG. 1. A perspective view of the rotating cell. The inset shows the speed of motor.

such multiple measurements, at various  $p/p_0$  during adsorption and desorption, the adsorption isotherm can be recovered from the SAXS data, the existence of network effects can be considered, and the size of internal surface rugosity (if any) can be estimated from the thickness of the adsorbed film (defractalization).<sup>20</sup>

However, adsorption *in situ* with SAXS remains a static technique, where spectra are recorded in an equilibrium condition. In this work, a new sample cell that allows adsorption in conjunction with x-rays under a rotational field is presented for the first time. This advancement will permit to examine the dynamic behavior of the liquid/vapor interface within the pore matrix at a given  $p/p_0$ . Four techniques will thus converge simultaneously (*in situ*) to the spectrum: (a) SAXS, (b) adsorption, (c) contrast matching, and (d) rotation. Rotation is expected to squeeze the adsorbed film toward the pore walls and consequently to increase  $I(Q)$ . The behavior of the liquid/vapor interface can be assessed too.

## DESIGN

Figure 1 shows the rotating sample cell. The cell has a light path difference of  $\sim 1$  mm in thickness. Apertures are covered with Mylar sheets. A hole that ends to the internal of the cell allows vapors from a distance reservoir to come, through an interchangeable tube connected with a pressure transducer, in contact with the sample under investigation at a specific  $p/p_0$  each time. In this way, adsorption in conjunction with SAXS, at various  $p/p_0$ , may be attained as a batch process.

The device consisted of a motor that rotates (up to 3000 rpm) the two gears in the back of the sample cell by a driving belt. The inset in Fig. 1 shows the relation between voltage and revolutions per minute (rpm). All mechanical parts are precisely manufactured in order to avoid vibrations. However, above 3000 rpm, there are vibrations that will affect the statistics of the spectrum.

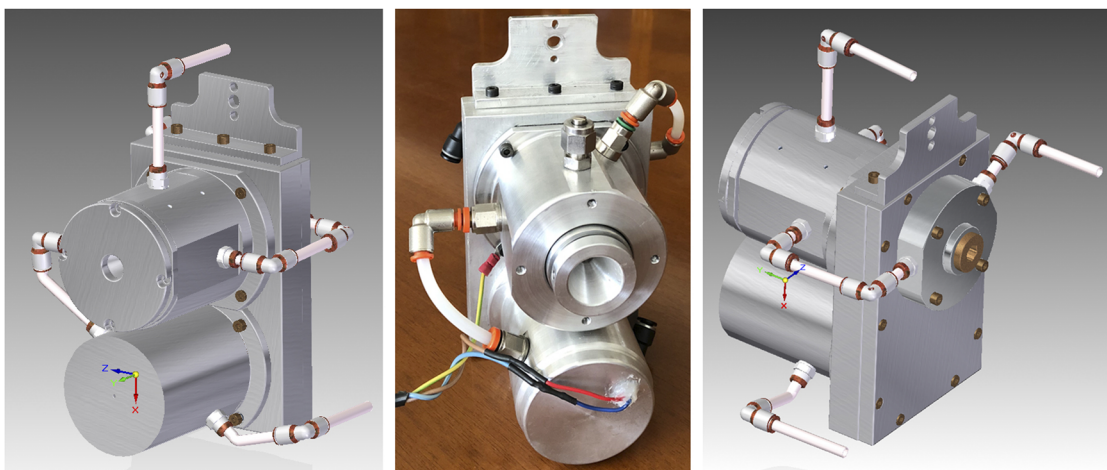


FIG. 2. The cooling system of the device; left: front view, right: back view, and middle: real view.

A cooling jacket with an internal flow system around the sample chamber and the motor, connected to a temperature controlled bath, is also constructed. When the isothermal temperature is established, a continuous flow ensures an error of not more than  $\pm 0.2$  °C. Figure 2 illustrates the cooling system and the adsorption tube of the device. Since the thickness of the beam line is 1 mm, the rotation method can easily interchange from homocentric to eccentric, by just moving the cell a few mm away from the beam line.

### Experimental details

Scattering experiments were conducted with a Rigaku S-Max3000 pinhole SAXS camera with Osmic Confocal Max-Flux optics.<sup>21</sup> This 3-pinhole system, adjusted in size and position, can shape the beam thickness to 1 mm. A 2D multiwire detector, of 120 mm diameter, was placed behind the sample cell at a sample-to-detector distance of 2593 mm. Measurements were carried out in a  $Q$  range of  $0.004 < Q < 0.1$  Å<sup>-1</sup>. The x-rays were produced by a Cu ( $\lambda = 1.54$  Å) rotating anode operated at 40 kV and 40 mA. The centre of the beam was calibrated with the diffraction peak of Ag-behenate

at  $d_{001} = 58.38$  Å. The data were corrected for dark current and empty tube scattering.

A disk of Vycor 7930 sample of 0,116 g weight, with 1 mm thickness and 1 cm diameter, was used in the present study. The sample was cleaned by immersion in 30% hydrogen peroxide and exposed to oxygen at 350 °C for 24 h. Dibromomethane (CH<sub>2</sub>Br<sub>2</sub>), which has a similar electron density as Vycor, was adsorbed at an isothermal temperature of 20 °C. Three spectral measurements were recorded with the aforementioned rotating cell as follows: (a) at  $p/p_0 = 0$  (i.e., dry sample) without rotation, (b) at  $p/p_0 = 0.5$  (i.e., partially loaded sample) without rotation, and (c) at  $p/p_0 = 0.5$  (i.e., same as previous) under rotation at an angular velocity  $\Omega = 2150$  rpm. From adsorption isotherm data, presented elsewhere,<sup>22</sup> the amount adsorbed at  $p/p_0 = 0.5$  was recorded equal to 60.7 mm<sup>3</sup>/g and is located at the lower closed point of the hysteresis loop.

Small angle x-ray scattering data were recorded by a homocentric operation of the cell, i.e., the beam line was coincided with the axis of rotation. This operation is the best choice for the given experiment because it provides an unchanged situation that facilitates comparison between the static and rotated spectra. That is, in all three cases, would be resulted to record the scattered intensities of the same pore domains,

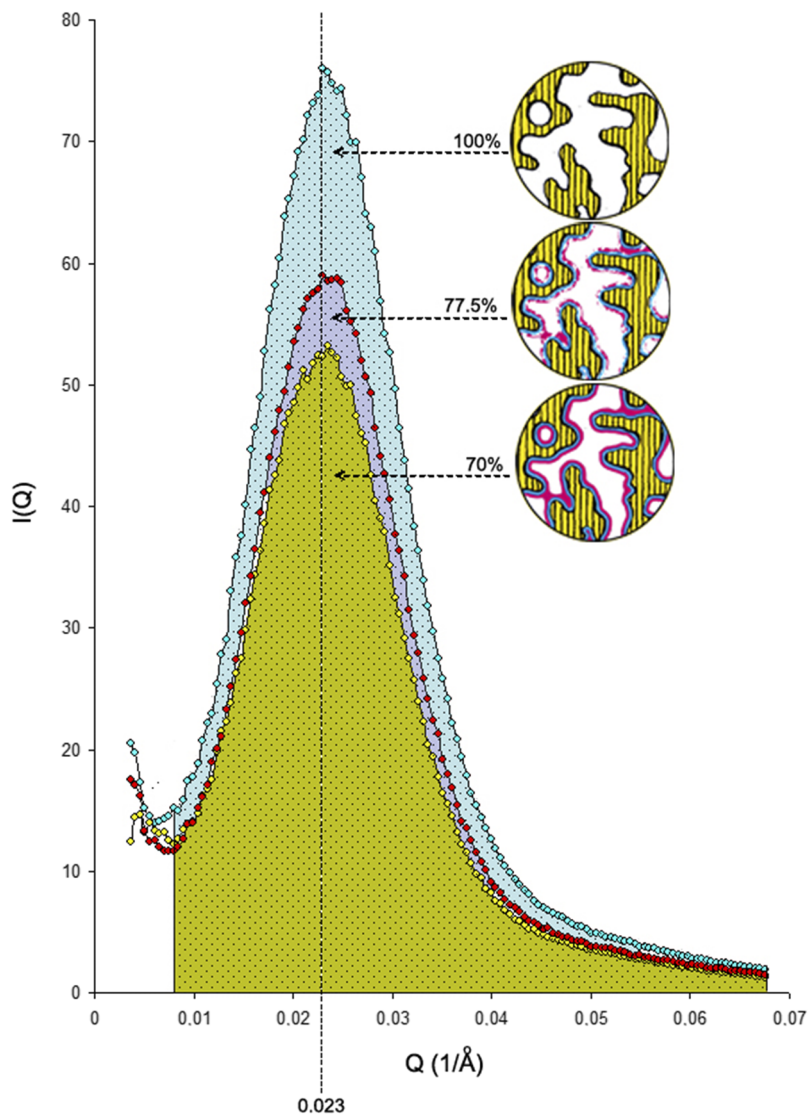


FIG. 3. Scattered intensity curves for three situations: cyan (upper curve) at  $p/p_0 = 0$  without rotation; yellow (lower curve) at  $p/p_0 = 0.5$  without rotation; and red (middle one) at  $p/p_0 = 0.5$  under rotation. Rotation recovers about 7.5% of the condensed space in the statistic situation; percentages for each case are shown too. The inset circular figures depict the possible mechanism for each situation. For sample loaded at  $p/p_0 = 0.5$  (lower figure), a two-layer adsorbed film of different heat of adsorption is considered, depicted in cyan and red. For the rotating sample (middle figure) at the same  $p/p_0$ , asymmetric ripples are introduced to the drawing; more space and more rugosity are assumed. The dry sample (upper figure) is illustrated as a reference.

whereas eccentric operation of the cell would be resulted to record  $I(Q)$  of different pore domains and at different initial and final positions.<sup>23</sup>

## MEASUREMENTS

Figure 3 shows the scattering intensity curves for all three cases, i.e., one with and two without rotation. The characteristic spinodal peak<sup>24</sup> of Vycor is located, as expected, at  $Q = 0.023 \text{ \AA}^{-1}$ , which corresponds to a Bragg spacing of  $273 \text{ \AA}$ . By calculating the area  $A_x$  under the scattering curves at a given  $x = p/p_0$ ,

$$A_x = \int_0^Q I(Q) dQ, \quad (3)$$

the following result is obtained:  $A_{0.5} < {}^{\text{ROT}}A_{0.5} < A_0$ . At low  $Q$  values, there is a drift in  $I(Q)$  due to rotation. In order to avoid any systematic error, the evaluation of  $A_x$  is limited at  $Q \geq 0.008 \text{ \AA}^{-1}$ . At high  $Q$  values, there is no substantial difference beyond  $Q \geq 0.0675 \text{ \AA}^{-1}$ .

At  $p/p_0 = 0.5$  in a static condition, the spectrum loses about 30% of its intensity relative to the dry sample ( $p/p_0 = 0$ ). During rotation, at  ${}^{\text{ROT}}p/p_0 = 0.5$ , the adsorbed film is pushed closer to pore walls. As a result, more space becomes available; hence,  $I(Q)$  increases by about 7.5%. Figure 4 demonstrates this course of events. In multilayer adsorption without rotation, the adsorbed molecules acquire a regular packing of thickness  $t_{\text{rp}} = 2R$  where  $R$  is the radius of the admolecule. Under rotation, a closer packing arrangement, which is thermodynamically more stable, may be obtained,  $t_{\text{cp}} = \sqrt{3}R < t_{\text{rp}}$ .<sup>25</sup> By assuming cylindrical pores of average radius<sup>26</sup> of about  $35 \text{ \AA}$ , a volume difference of 7.2% can be shown, which is very close to the value obtained from SAXS data. Again, our result is in accordance with the result of Yang *et al.*<sup>27</sup> who studied liquid holdup in a rotating packed bed using x-rays; that is, high rotational speed improves the distribution of liquid in the packing.

Figure 5 shows the decay of the scattered intensities at the Porod region, in a log-log plot. For each case, the following fractal dimensions were calculated:  $D_0 = 2.6$ ,  $D_{0.5} = 2.5$ , and  ${}^{\text{ROT}}D_{0.5} = 2.8$ . Although the decrease in  $D$

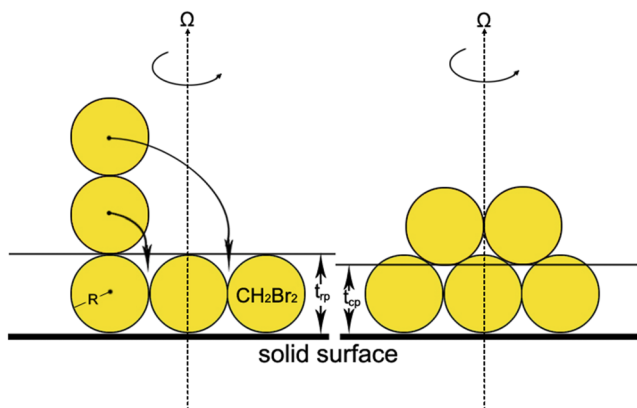


FIG. 4. Schematic illustration of the effect of rotation on the adsorbed film. Admolecules have a different packing arrangement before rotation and during rotation of angular velocity  $\Omega$ . The motion of the molecules is shown by the solid arrows.

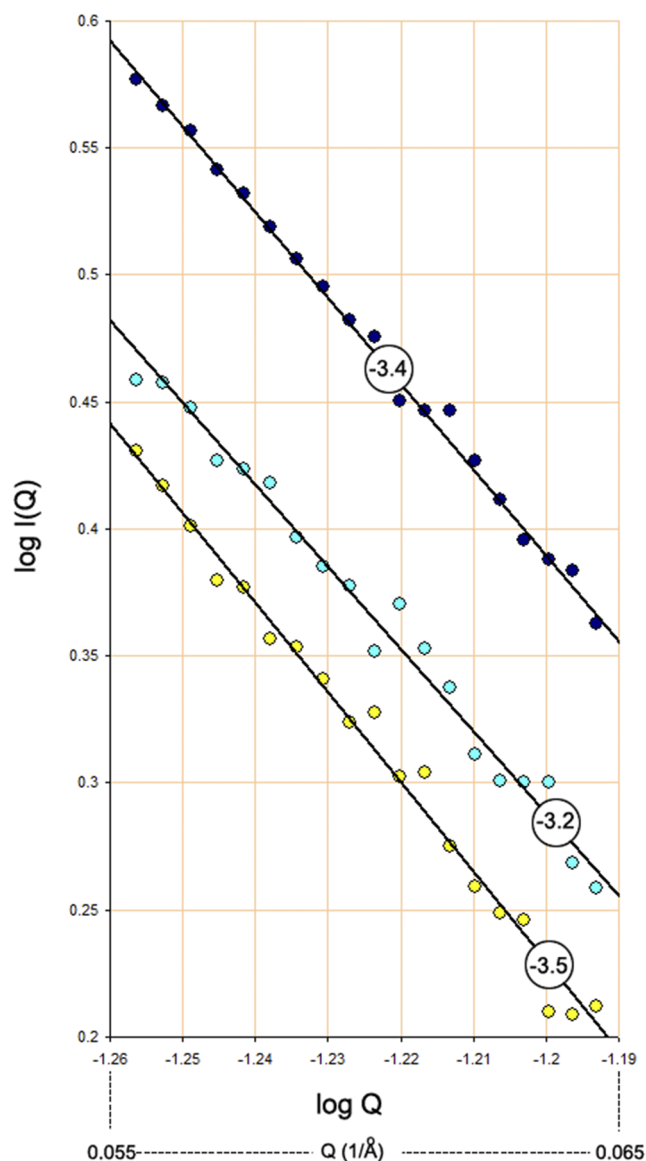


FIG. 5. Log-log plot for the three situations. The fractal dimensions were calculated from the slopes of the lines equal to  $D_0 = 2.6$  for the dry sample and  $D_{0.5} = 2.5$  for the loaded one. Under rotation, the loaded sample shows an abnormal fractal dimension of  ${}^{\text{ROT}}D_{0.5} = 2.8$ . It was concluded that the rotation creates asymmetric ripples on the liquid/vapor interface.

between  $p/p_0 = 0$  and  $p/p_0 = 0.5$  is related to a defractalization process, the increase in  $D$  during rotation implies a different mechanism. According to Brunauer-Emmet-Teller (BET) theory<sup>28</sup> for multilayer adsorption, in all layers, except the first, the heat of adsorption is equal to the molar heat of condensation. Based on previous experimental values<sup>22</sup> of the Halsey-type equation for  $\text{CH}_2\text{Br}_2$ , at  $p/p_0 = 0.5$ , a statistical film of about two layer thickness is inferred. During rotation, the liquid/vapor interface develops asymmetric ripples that influence the decay of  $I(Q)$  at high  $Q$  values. As a result, an enhanced artificial roughness is measured by the instrument. The insets in Fig. 3 depict this situation.

## CONCLUSIONS

A rotating sample cell for studies of adsorption *in situ* with SAXS is presented. The device allows dynamic

phenomena that take place at nanoscale to be measured and quantify. This option is very important in material's characterization with SAXS which so far is limited to static examination of the interfacial liquid. In general, rotation can provide information on the behavior of a fluid within a porous system, e.g., pore and surface diffusion and capillary condensation flow. Although transport phenomena are commonly related to a linear rather than to a radial direction, the resemblance of kinetic to rotation energy provides a reliable framework for evaluating them. As an example, in this work, the motion of admolecules at the liquid-liquid and gas-liquid interfaces was examined and quantified.

## ACKNOWLEDGMENTS

The authors R.I.K., G.A.B., E.P.F., and A.Ch.M. would like to thank the project entitled "*CO<sub>2</sub> separations by using mixed matrix, based on nano-carbon materials, membranes*" /GG-CO<sub>2</sub>, T2ΔΓE-0183 for the partial funding of this work. E. P. Favvas would also like to acknowledge the support of the project MIS 5002567, implemented under the "*Action for the Strategic Development on the Research and Technological Sector*," funded by the Operational Programme "*Competitiveness, Entrepreneurship and Innovation*" (NSRF 2014–2020) and co-financed by Greece and the European Union (European Regional Development Fund). The author A. Ch. M. would like to thank the project entitled "*Development of NAnotechnology-enabled "next-generation" MEmbranes and their applications in Low-Energy, zero liquid discharge Desalination membrane systems*" /NAMED, T2ΔΓE-0597 for funding.

<sup>1</sup>C. Ramshaw and R. H. Mallinson, "Mass transfer process," U.S. patent 4,283,255 (11 August 1981).

<sup>2</sup>S. Munjal, M. P. Dudukovic, and P. Ramachandran, *Chem. Eng. Sci.* **44**, 2257 (1989).

<sup>3</sup>T. Kelleher and J. R. Fair, *Ind. Eng. Chem. Res.* **35**, 4646 (1996).

<sup>4</sup>C. C. Lin and H. S. Liu, *Ind. Eng. Chem. Res.* **39**, 161 (2000).

<sup>5</sup>C. Zheng, K. Guo, Y. Feng, and C. Yang, *Ind. Eng. Chem. Res.* **39**, 829 (2000).

<sup>6</sup>Y. S. Chen and H. S. Liu, *Ind. Eng. Chem. Res.* **41**, 1583 (2002).

<sup>7</sup>D. P. Rao, A. Bhowal, and P. S. Goswami, *Ind. Eng. Chem. Res.* **43**, 1150 (2004).

<sup>8</sup>Y. S. Chen, F. Y. Lin, C. C. Lin, C. Y. D. Tai, and H. S. Liu, *Ind. Eng. Chem. Res.* **45**, 6846 (2006).

<sup>9</sup>M. S. Jassim, G. Rochelle, D. Eimer, and C. Ramshaw, *Ind. Eng. Chem. Res.* **46**, 2823 (2007).

<sup>10</sup>T. van Gerven and A. Stankiewicz, *Ind. Eng. Chem. Res.* **48**, 2465 (2009).

<sup>11</sup>L. M. de Socio, N. Ianiro, and L. Marino, *J. Thermophys. Heat Transfer* **14**, 269 (2000).

<sup>12</sup>V. I. Geyko and N. J. Fisch, *Phys. Rev. Lett.* **110**, 150604 (2013).

<sup>13</sup>X. Gao, G.-W. Chu, Y. Ouyang, H. Zou, Y. Luo, Y. Xiang, and J.-F. Chen, *Ind. Eng. Chem. Res.* **56**, 14350 (2017).

<sup>14</sup>A. Guinier and G. Fournet, *Small-Angle Scattering of X-Rays* (John Wiley and Sons, New York, 1955).

<sup>15</sup>H. D. Bale and P. W. Schmidt, *Phys. Rev. Lett.* **53**, 596 (1984).

<sup>16</sup>A. C. Mitropoulos, J. M. Haynes, R. M. Richardson, and N. K. Kanellopoulos, *Phys. Rev. B* **52**, 10035 (1995).

<sup>17</sup>E. Hoinkis, *Part. Part. Syst. Charact.* **21**, 80 (2004).

<sup>18</sup>G. H. Findenegg, S. Jahnert, D. Muter, J. Prass, and O. Paris, *Phys. Chem. Chem. Phys.* **12**, 7211 (2010).

<sup>19</sup>A. C. Mitropoulos, *J. Colloid Interface Sci.* **317**, 643 (2008).

<sup>20</sup>E. Cheng, M. W. Cole, and P. Pfeifer, *Phys. Rev. B* **39**, 12962R (1989).

<sup>21</sup>See [www.axt.com.au](http://www.axt.com.au) for Rigaku S-Max3000 Pinhole Camera Small Angle X-Ray Scattering system brochure.

<sup>22</sup>A. C. Mitropoulos, *J. Colloid Interface Sci.* **336**, 679 (2009).

<sup>23</sup>Eccentric rotation will average  $I(Q)$  of pore domains found on the perimeter  $2\pi k_e$ , where  $k_e$  is the distance between the beam line and the axis of rotation.

<sup>24</sup>P. Wiltzius, F. S. Bates, S. B. Dierker, and G. D. Wignall, *Phys. Rev. A* **36**, 2991R (1987).

<sup>25</sup>S. J. Gregg and K. S. W. Sing, *Adsorption, Surface Area and Porosity* (Academic Press, London, 1982).

<sup>26</sup>A. C. Mitropoulos, K. L. Stefanopoulos, E. P. Favvas, E. Vansant, and N. P. Hankins, *Sci. Rep.* **5**, 10943 (2015).

<sup>27</sup>Y. Yang, Y. Xiang, G. Chu, H. Zou, Y. Luo, M. Arowo, and J.-F. Chen, *Chem. Eng. Sci.* **138**, 244 (2015).

<sup>28</sup>S. Brunauer, P. H. Emmett, and E. Teller, *J. Am. Chem. Soc.* **60**, 309 (1938).